Journal Pre-proof

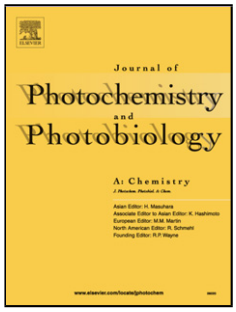

Advanced oxidation processes for elimination of xylene from waste gases

Tomáš Prostějovský, Martin Reli, Radim Žebrák, Tereza Konečná, Federico Salvadores, Milagros M. Ballari, Kamila Kočí

PII: S1010-6030(20)30844-3

DOI: https://doi.org/10.1016/j.jphotochem.2020.113047

Reference: JPC 113047

To appear in: *Journal of Photochemistry & Photobiology, A: Chemistry*

Received Date: 29 May 2020

Revised Date: 12 November 2020

Accepted Date: 13 November 2020

Please cite this article as: Prostějovský T, Reli M, Žebrák R, Konečná T, Salvadores F, Ballari MM, Kočí K, Advanced oxidation processes for elimination of xylene from waste gases, *Journal of Photochemistry and amp; Photobiology, A: Chemistry* (2020), doi: https://doi.org/10.1016/j.jphotochem.2020.113047

Advanced oxidation processes for elimination of xylene from waste gases

Tomáš Prostějovský[a,b,1*], Martin Reli[b,2], Radim Žebrák[c,3], Tereza Konečná[c,4], Federico Salvadores[d,5], Milagros M. Ballari[d,6], Kamila Kočí[b,7]

[a]Faculty of Materials Science and Technology, VŠB – Technical University of Ostrava, 17. listopadu 2172/15, Ostrava-Poruba, 708 00, Czech Republic

[b]Institute of Environmental Technology, VŠB – Technical University of Ostrava, 17. listopadu 2172/15, Ostrava-Poruba, 708 00, Czech Republic

[c]Dekonta Inc., Dřetovice 109, Stehelčeves, 273 42, Czech Republic

[d]INTEC (Universidad Nacional del Litoral and CONICET), Ruta Nacional Nº 168., 3000 Santa Fe, Argentina

[1*]E-mail: tomas.prostejovsky@vsb.cz, Phone: +420 597 326 556

[2]Email: martin.reli@vsb.cz

[3]E-mail: zebrak@dekonta.cz

[4]E-mail: tereza.konecna@dekonta.cz

[5]E-mail: fsalvadores@intec.unl.edu.ar

[6]E-mail: ballari@santafe-conicet.gov.ar

[7]E-mail: kamila.koci@vsb.cz

Graphical_Abstract

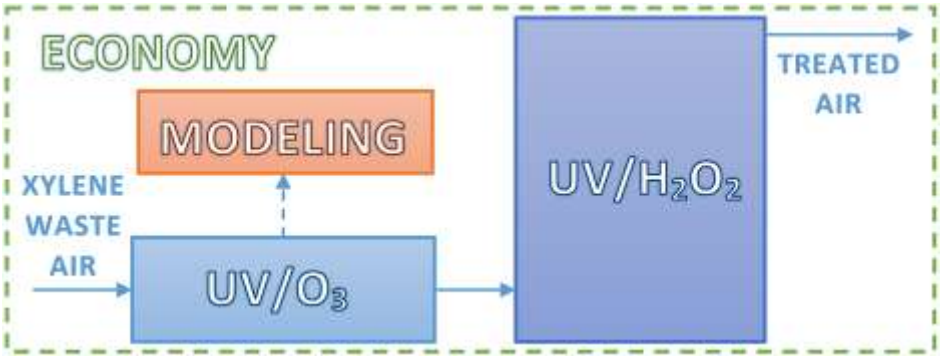

Highlights

- 2 stage AOP pilot plant unit for the elimination of VOCs from waste air
- 1st photolytic stage utilizes UV/O_3 and 2nd photochemical stage utilizes UV/H_2O_2
- Mathematically modeled 1st stage correlate with experimental data
- Final xylene conversion strongly depends on initial concentration and flow rate
- Figures-of-merit proved using both stages is more economically advantageous

Abstract

The elimination of xylene was experimentally studied using advanced oxidation process in a two-step pilot plant photochemical unit with the use of UV irradiation combined with ozone (first step) and with hydrogen peroxide solution (second step). The influence of the initial xylene concentration and air flow rate was investigated. A mathematical model of the first step of the unit applying UV/O_3 treatment was developed. Xylene conversion decreased with increasing its initial concentration and increasing flow rate of the air (lowering residence time in the unit). The highest xylene conversion (95 %) was achieved with the initial concentration

50 ppmv and the flow rate 57 $m^3 \cdot h^{-1}$. Based on the model results for the first photolytic step of the pilot plant unit, the main pathway of the elimination of xylene is its reaction with hydroxyl radicals which are formed both by the reaction of ozone with water/humidity but also by the reaction of singlet oxygen (formed by the decomposition of ozone) with water/humidity. Calculated figures-of-merit showed that the pilot plant unit is more energy-cost-efficient for the higher flow rates of the waste gas. The technology using advanced oxidation processes seems promising for the elimination of organic compounds from the air, although further studies are necessary.

Keywords: Advanced oxidation processes, Xylene, UV irradiation, Ozone, Hydrogen peroxide

1. Introduction

With the scientific world searching for the effective, economic and green-way methods for the dealing with the impact of the humankind on the environment, advanced oxidation processes (AOPs) have come to the spotlight. AOPs cover a wide area of methods that use both chemical and physical principles in dealing with the pollutants. Nevertheless, the main use of AOPs these days is in the water treatment [1-4], because of the easy generation of hydroxyl radicals, that are the main oxidation agents in AOPs. But treating the polluted air is also possible and extensively studied [5-7].

The issue of pollutants present in the environment is being increasingly studied. Studies prove that volatile organic compounds (VOCs) play a major role in reactions that lead to raising concentrations of tropospheric ozone, mainly in the recent years. As a part of photochemical smog (the Los Angeles type) VOCs have negative effect not only on the human health, but also on the environment and urban buildings [8, 9]. Needless to say, traffic is not the only source of VOCs. Many of them are also well known and widely used as an industrial solvents

and also raw materials for the production of polymers. For example, xylene (as a mixture of its three isomers) is a solvent with use in printing, rubber, leather and petrochemical industries [8, 10].

Main symptoms of short term exposure to xylene are eye, nose and throat irritation and breathing and nervous system problems [11]. Long term exposure can lead to severe problems like lung cancer, anemia, leukemia, etc. [12].

Governments all around the world are lowering exposure limits for VOCs in general. The Czech legislative states that xylene, as a part of VOCs sum, should not exceed 150 mg $\cdot$ m^{-3} in the outlet air (around 35 ppm). These low limits are starting to cause an issue because these days, technologies for the removal of VOCs are starting to become insufficient in terms of availability and dimensions of the devices itself. One of these technologies are biofilters. They can provide high removal efficiency coming hand in hand with low cost of the treatment, with the disadvantage mentioned above, their big dimensions [13-15]. Other way can be catalytic combustion of VOCs [16, 17]. This method can achieve high efficiency, but deals with higher energy demand with possible problems with catalyst leak to the environment. Also quite common is the use of adsorption process, often carried out on the activated carbon [18-20]. Disadvantage of this technology is further desorption of VOCs and possible regeneration of the activated carbon.

This work aims to the use of strong ultraviolet (UV) irradiation in combination with ozone and hydrogen peroxide for treating the waste gas stream in higher flows to simulate real conditions in industry. In comparison to other studies [21-23] this work uses no catalyst to achieve low costs and high efficiency of the removal of xylene.

2. Materials and Methods

Xylene oxidation experiments were conducted in a two-step unit apparatus. The first step (R1, UV/O_3) was a continuous flow photolytic reactor (Figure 1 and 2) made from stainless steel of internal volume 2.45×10^{-1} m^3. It had a square cross-profile of 0.35 × 0.35 m and length 2 m. Sixteen UV lamps with peak intensities at λ = 254 nm and 185 nm (80 W, UVC-80 W T5 4P/O3, UVC Servis Ltd.) were used. These lamps were implemented in the reactor chamber in two horizontal planes separated by a 0.05 m gap and which were in a 0.13 m distance from the upper and lower wall of the reactor chamber. Lamps in each plane were 0.08 m apart from each other. Four darkened glass windows were placed on the top side of the reactor for the optical control of the reactor chamber. The relative humidity of the inlet gas was 50 % and the average temperature inside the reactor was 29°C. The concentration of ozone produced by the UV lamps was measured by Gas Detector WASP-XM with portable pump-suction gas detector (Hunan GRI Instrument CO., Ltd.). Radiation intensities of the lamps at 254 nm were measured by UVA/UVC Light Meter/Datalogger (SDL470, Extech instruments).

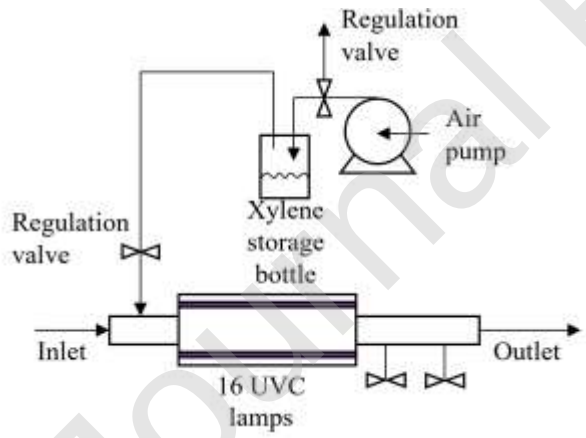

Figure 1 Scheme of the photolytic reactor with dosing of xylene.

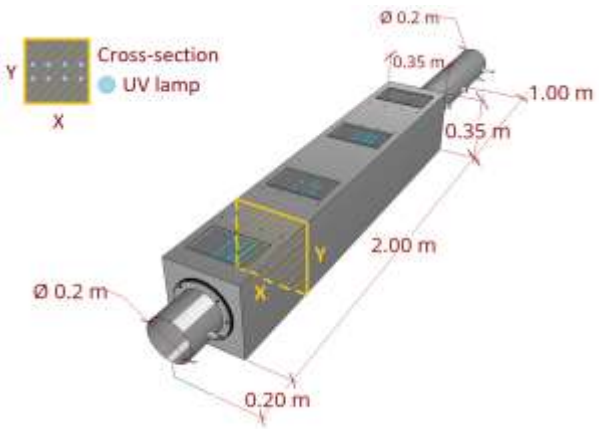

Figure 2 Drawing of the photolytic reactor with highlighted cross-section.

The second step (R2, UV/H_2O_2) of the apparatus consisted of a continuous flow photochemical reactor (Figure 3) made from high-density polyethylene (HDPE). Internal irradiated volume was 2.28 m^3. Fifteen UV lamps (λ = 254 nm, 75 W, TUV 64 T5 4P-SE 75W UVC, Philips) were placed inside the reactor cross-wise and were divided into 3 sections that could be switched on separately. It is worth to mention that these lamps do not produce ozone. There was a storage tank (3.0×10^{-1} m^3) at the bottom of the reactor with water solution of hydrogen peroxide (c = 0.1 mol · dm^{-3}). This hydrogen peroxide solution was pumped and sprayed through 6 showers heads in the upper part of the reactor. Hydrogen peroxide concentrations were determined manganometrically by adding potassium permanganate solution to the liquid sample with addition of sulfuric acid and manganese sulfate monohydrate solution. There is a filling layer between the irradiated section and the storage tank. Another four lamps were placed directly in the water storage tank, but these were turned on after the experiment to get rid of any organics that was dissolved in the hydrogen peroxide solution during the run of the experiment.

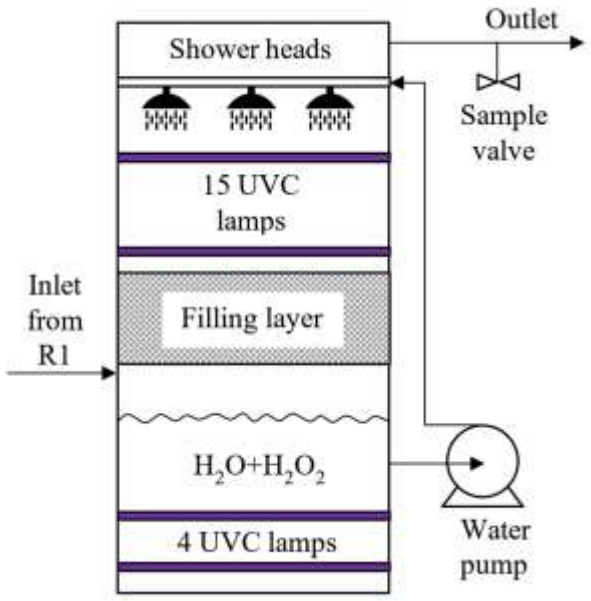

Figure 3 Scheme of the photochemical reactor.

Dosage of xylene was assured by blowing air through the storage bottle with liquid xylene (mixture of isomers, p.a.) and then the air with xylene vapors was driven to the inlet of the photolytic reactor. Concentrations of xylene were set by modifying the amount of air driven to the storage bottle. Samples of the waste air were analyzed using a gas chromatograph Young Lin YL6100GC equipped by FID. Gas chromatograph with quadrupole mass selective detector (GC 7890 + MSD 5975, Agilent) was used to determine all the products both in the outlet air and in the hydrogen peroxide solution. The dependence of conversion of xylene on its initial concentration and the flow rate of the waste air was tested individually in the first step (R1) and in both steps (R1+R2) connected in series.

Experiments were conducted with four different initial concentrations of xylene (50; 100; 150; 200 ppmv) and two different flow rates (57 and 113 $m^3 \cdot h^{-1}$). Gas samples of the contaminated air were taken at the outlet from the R2 after each step influencing the concentration of xylene. There were at least 30 minutes after each part was turned on so the

equilibrium could be achieved. For the first experiment setup mentioned above the steps influencing the outlet concentration of xylene were as follows:

- turning on the air pump for the dosing of xylene,
- turning on 16 lamps in R1.

Following steps came with the second experimental setup:

- turning on the water pump for the circulation of hydrogen peroxide solution in R2,
- turning on 15 lamps in R2.

At the end of the experiment everything was turned off except the air pump so the stability of the inlet concentration of xylene could be tested.

Effectivity of the elimination of xylene was evaluated as conversion of xylene from the experimental data according to the Equations (1) and (2),

$$X_{xyl} = \frac{n_{xyl,0} - n_{xyl}}{n_{xyl,0}} \quad (1)$$

$$X_{xyl} = \frac{c_{xyl,0} - c_{xyl}}{c_{xyl,0}} \qquad V = \text{const.} \quad (2)$$

where X_{xyl} is the degree of conversion (-), $n_{xyl,0}$ is the initial substance amount of xylene (mol), n_{xyl} is the substance amount of xylene at the set time (mol). In the case of constant volume, $c_{xyl,0}$ is the initial concentration of xylene (ppmv) and c_{xyl} is the concentration of xylene at the set time (ppmv).

3. Results and Discussion

3.1 Elimination of xylene in the photolytic reactor (UV/O_3)

The oxidation of xylene in the first step (photolytic reactor, R1) is based on the interaction between UV and ozone. The ozone is produced from the UV lamps present in the reactor. They provide strong UV irradiation (185/254 nm) which reacts with oxygen molecule in the air and two oxygen atoms are formed (Equation (3)). These atoms then react with oxygen molecule and ozone is produced (Equation (4)) [24].

$$O_2 \xrightarrow{h\nu\ (185\ nm)} 2O \quad (3)$$

$$O + O_2 \rightarrow O_3 \quad (4)$$

Ozone concentrations were measured during experimental runs at the output from R1 and varied from 25 to 230 ppmv depending on the actual flow rate of the waste air through the unit (Tables 1 and 2).

Table 1 Dependency of ozone concentration on the air flow rate and initial xylene concentration after turning R1.

R1 ON					
	Initial (set) concentration of xylene (ppmv)				
	0	50	100	150	200
Air flow ($m^3 \cdot h^{-1}$)	**Steady-state concentration of ozone (ppmv)**				
57	230	150	130	77	45
113	170	108	60	55	25

Table 2 Dependency of concentration on the air flow rate and initial xylene concentration after both reactors (R1+R2) were turned on.

R1+R2 ON				
	Initial (set) concentration of xylene (ppmv)			
	50	100	150	200
Air flow ($m^3 \cdot h^{-1}$)	**Steady-state concentration of ozone (ppmv)**			
57	35	25	15	9

113	35	20	10	8

It is possible that oxygen radicals and ozone could attack xylene molecule, mainly the substituent groups, producing higher oxidized forms of xylene such as carboxylic acids or even carbon dioxide and water. Oxidation of pollutant is not the only consumption of ozone in the reactor, the other way ozone is consumed is by reacting with UV irradiation < 328 nm. According to Munter [25] this reaction provides a highly reactive singlet oxygen atom $O(^1D)$ and an oxygen molecule (Equation (5)). The singlet oxygen atom can react with water vapor present in the air and produce two hydroxyl radicals $OH^{\bullet}$ (Equation (6)).

$$O_3 \xrightarrow{h\nu} O_2 + O(^1D) \quad (5)$$

$$O(^1D) + H_2O \rightarrow 2OH^{\cdot} \quad (6)$$

Johnson et al. [26] suggested that $O(^1D)$ can also react with present organic compound resulting in production of $R^{\bullet}$ and $OH^{\bullet}$ radicals (Equation (7)). Lastly the singlet oxygen atom can react with many molecules present in the air (N_2, Ar, CO_2 etc.) producing a ground state oxygen $O(^3P)$ (Equation (8)), which can react with molecular oxygen and produce ozone (Equation (9)).

$$O(^1D) + RH \rightarrow R^{\cdot} + OH^{\cdot} \quad (7)$$

$$O(^1D) + M \rightarrow O(^3P) + M \quad (8)$$

$$O(^3P) + O_2 + M \rightarrow O_3 + M \quad (9)$$

where M = N_2, Ar, CO_2 etc.

The formed hydroxyl radicals can oxidize the VOCs either through addition into an unsaturated VOC or by removal of hydrogen (Eq. (10) and (11)), but the removal of hydrogen is the less probable reaction (less than 10 % of the overall reaction pathway [27]).

$$OH^{\cdot} + RH \rightarrow \text{adduct} \quad (10)$$

$$OH^{\cdot} + RH \rightarrow H_2O + R^{\cdot} \quad (11)$$

The organic radical is afterwards oxidized into several intermediates and stable products. Generally, there are three mechanisms of the oxidation of VOCs, oxygen addition, splitting of the molecule into smaller fragments (CO, CO_2, HCHO, HCOOH) and oligomerization.

Hydroxyl radicals are another important oxidation agents in AOPs, several studies report their reactions with xylene [28-31].

Simply said, the oxidation of organic molecule in the photolytic reactor is caused by several oxidation agents, ozone, oxygen radical, hydroxyl radical and singlet oxygen. In case of generating hydroxyl radicals in the air, only 10 % of the $O(^1D)$ atoms reacts with water vapor and makes $OH^{\bullet}$ radicals (even at 100% humidity). 90 % of them decay into $O(^3P)$ (Equation (8)) [32]. In addition, water photolysis at 185 nm is a source of hydroxyl radicals [33]. The inlet air has 50% of relative humidity. This is equal to 3.85×10^{17} molecules $\cdot$ cm^{-3}, which could lead to an important generation of $OH^{\bullet}$ radicals. On the other hand, the reaction pathway of xylene with $OH^{\bullet}$ radicals is widely documented in literature [34-36].

Figure 4 shows a comparison of conversions in dependence on the flow rate and initial concentration of xylene after passing through the photolytic reactor. It is clear that at lower flow rates the conversion is higher, mainly due to the longer residence time (approx. 15.6 s for the flow rate 57 $m^3 \cdot h^{-1}$ in comparison with 7.8 s for the flow rate 113 $m^3 \cdot h^{-1}$). Simultaneously, higher conversion is achieved with lower initial concentrations of xylene. It

is also clear the conversion of xylene is becoming more or less the same (slightly above 10 %) with increasing initial concentration and flow rate.

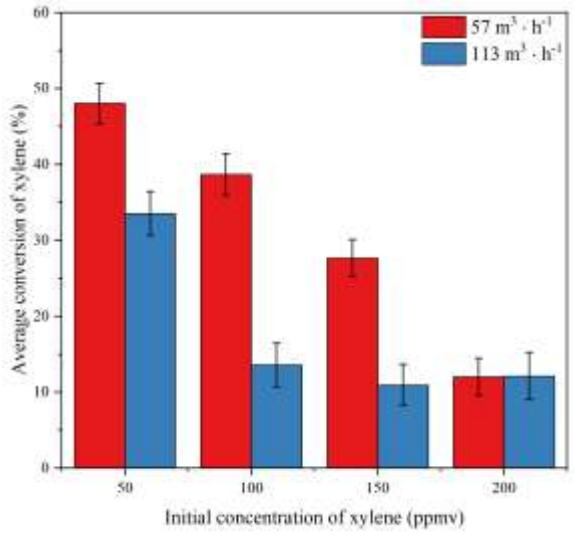

Figure 4 Comparison of average conversions of xylene after passing through the photolytic reactor (R1) at different initial concentrations of xylene and two different flow rates.

3.2 Elimination of xylene in both steps of the unit (UV/O_3 + UV/H_2O_2)

The second step (photochemical, R2) of the pilot plant experimental unit works as a wet scrubber for the polar compounds, ozone and carbon dioxide coming from the photolytic reactor. These compounds are being dissolved into the recirculating water. Therefore, the oxidation reactions are undergoing in gas phase and in the aqueous phase as well. Since the xylene has very low solubility in water (< 0.2 $g \cdot m^{-3}$ at 20°C) the oxidation of the not oxidized xylene from R1 is proceeding in gas phase. The same applies for any non-polar by-products produced in R1. The oxidation of these non-polar compounds is following the same steps as in R1 due to a still present ozone (not all ozone is being dissolved) and hydroxyl radicals coming from R1 along with the xylene. Additional hydroxyl radicals are produced from hydrogen peroxide present in recirculating water (Equation (12)). These are mainly responsible for oxidation of polar by-products dissolved in water in R2.

$$H_2O_2 \xrightarrow{h\nu\ (254\ nm)} 2OH^{\cdot} \quad (12)$$

Furthermore, hydroperoxyl anion, that is present because of its equilibrium with hydrogen peroxide, also absorbs UV irradiation at 254 nm, which is contra-productive because of lowering the production rate of hydroxyl radicals compared to the direct photolysis of H_2O_2 (Equation (13) and (14)) [25].

$$H_2O_2 \leftrightarrow HO_2^- + H^+ \quad (13)$$

$$HO_2^- \xrightarrow{h\nu\ (254\ nm)} OH^{\cdot} + O^- \quad (14)$$

Figure 5 shows an experimental run with initial concentration of xylene 150 ppmv and flow rate 57 $m^3 \cdot h^{-1}$. After setting the desired concentration, the 16 UV lamps in the photolytic reactor (R1) were turned on and a major decrease in xylene concentration was observed. Next, the circulation of water solution of hydrogen peroxide was turned on in R2. This step had no effect on the concentration of xylene due to a very low solubility of xylene in water. The second decrease in the xylene concentration was observed after the 15 lamps in the photochemical reactor (R2) were turned on. Mass spectroscopy proved that all conversed xylene was transformed into CO_2 and H_2O, because no products or by-products were detected either in the hydrogen peroxide solution nor in the outlet air. Comparison of average conversions in the unit at tested flow rates (Figure 6) shows high effectivity of the photochemical reactor. As expected, the average conversion is lower at the flow rate 113 $m^3 \cdot h^{-1}$ than at the flow rate 57 $m^3 \cdot h^{-1}$.

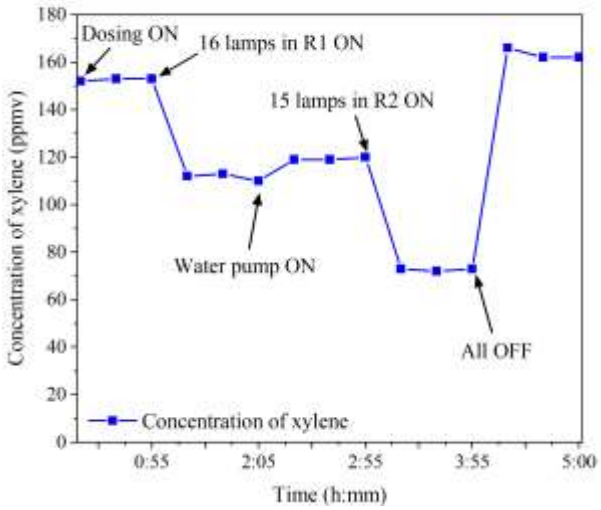

Figure 5 Time dependency of xylene concentration with initial concentration 150 ppmv and flow rate 57 $m^3 \cdot h^{-1}$.

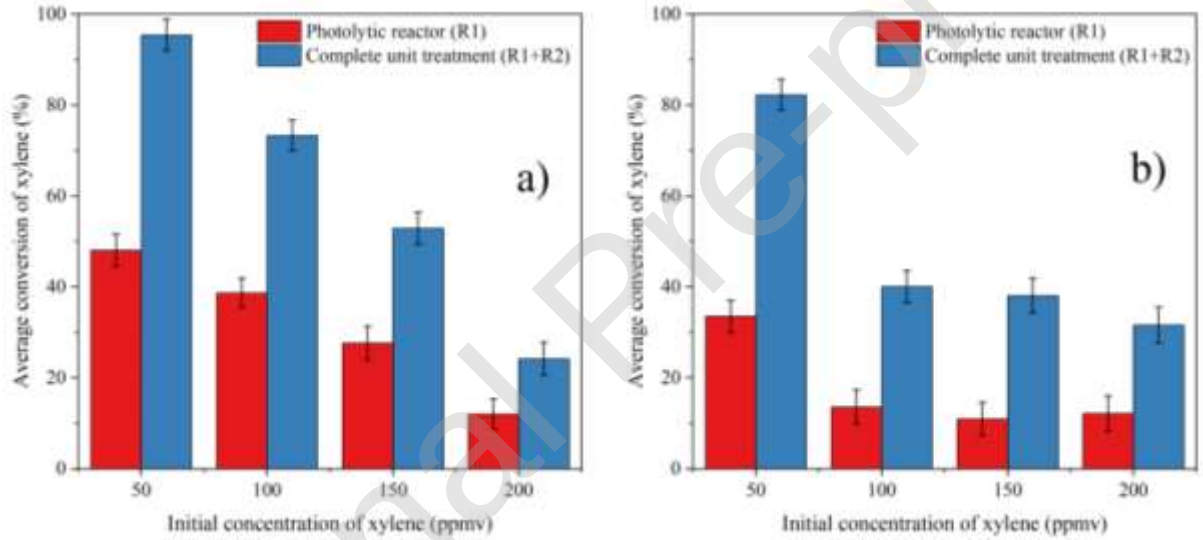

Figure 6 Comparison of average conversions of xylene after treatment in the photolytic reactor and after treatment at the whole unit at the flow rate a) 57 $m^3 \cdot h^{-1}$, b) 113 $m^3 \cdot h^{-1}$.

3.3 Mathematical modeling of the photolytic reactor (UV/O_3)

As a part of a better understanding of the ongoing processes in the photolytic reactor and further research, a simple mathematical model was proposed.

According to Burkholder et al. [33], Fan et al. [31] and Mohseni et al. [37], 48 possible reactions were proposed to happen in the photolytic reactor. Many of the reactions were

discarded because their reaction rate was many orders of magnitude lower than other reactions. In addition, the only considered compounds entering in the reactor were xylene, oxygen, water and nitrogen. State transfer reactions of oxygen atoms were also excluded because all of these forms were considered as simply O• radicals for the purpose of simplification of this model. Additionally, the photolysis of xylene at 254 nm is not possible according to our experiments (data not shown) and also as reported in Mohseni et al. [37]. On the other hand, Mohseni et al. [37] proved that photolysis of xylene is possible in a nitrogen atmosphere with 185 nm radiation. Thus, the final scheme of reaction for xylene decomposition and ozone generation in the reactor consisted of fourteen reactions (Equation (15)-(28)).

$$H_2O + h\nu_{185} \rightarrow OH^{\cdot} + H^{\cdot} \qquad r_1 = J_1[H_2O] \qquad (15)$$

$$O_2 + h\nu_{185} \rightarrow 2O^{\cdot} \qquad r_2 = J_2[O_2] \qquad (16)$$

$$O_3 + h\nu_{185} \rightarrow O_2 + O^{\cdot} \qquad r_3 = J_3[O_3] \qquad (17)$$

$$O_3 + h\nu_{254} \rightarrow O_2 + O^{\cdot} \qquad r_4 = J_4[O_3] \qquad (18)$$

$$xyl + h\nu_{185} \rightarrow products \qquad r_5 = J_5[xyl] \qquad (19)$$

$$xyl + OH^{\cdot} \rightarrow products \qquad r_6 = k_6[xyl][OH^{\cdot}] \qquad (20)$$

$$O^{\cdot} + O_3 \rightarrow 2O_2 \qquad r_7 = k_7[O^{\cdot}][O_3] \qquad (21)$$

$$O^{\cdot} + H_2O \rightarrow 2OH^{\cdot} \qquad r_8 = k_8[O^{\cdot}][H_2O] \qquad (22)$$

$$O^{\cdot} + OH^{\cdot} \rightarrow O_2 + H^{\cdot} \qquad r_9 = k_9[O^{\cdot}][OH^{\cdot}] \qquad (23)$$

$$H^{\cdot} + O_3 \rightarrow OH^{\cdot} + O_2 \qquad r_{10} = k_{10}[H^{\cdot}][O_3] \qquad (24)$$

$$OH^{\cdot} + O_3 \rightarrow products \qquad r_{11} = k_{11}[OH^{\cdot}][O_3] \qquad (25)$$

$$O^{\cdot} + O_2 + M \rightarrow O_3 + M \qquad r_{12} = k_{12}[O^{\cdot}][O_2][M] \qquad (26)$$

$$H^{\cdot} + O_2 + M \rightarrow \text{products} + M \qquad r_{13} = k_{13}[H^{\cdot}][O_2][M] \tag{27}$$

$$O^{\cdot} + N_2 + M \rightarrow N_2O + M \qquad r_{14} = k_{14}[O^{\cdot}][N_2][M] \tag{28}$$

where $r_{1\ldots14}$ are reaction rates (molecule $\cdot$ cm^{-3} $\cdot$ s^{-1}), $J_{1\ldots5}$ are photolysis rates for corresponding reactions (s^{-1}), $k_{6\ldots14}$ are reaction rate constants for corresponding reactions (cm^3 $\cdot$ molecule $\cdot$ s^{-1}), "a" stands for present compounds/radicals and [a] are concentrations of compounds/radicals (molecules $\cdot$ cm^{-3}), "M" represent any molecule present in the air, and [M] is the Loschmidt number, that for air can be considered equal to 2.5×10^{19} molecule $\cdot$ cm^{-3}.

Photolysis rates $J_{1\ldots5}$ were determined according to Equation (29),

$$J_n = \int_{\lambda} F_{\lambda}\, \sigma_{a,\lambda} \Phi_{a,\lambda} d\lambda \tag{29}$$

where J_n is the photolysis rate for the "a" compound (s^{-1}), F_{λ} is the spectral actinic flux (photons $\cdot$ cm^{-2} $\cdot$ s^{-1} $\cdot$ nm^{-1}), $\sigma_{a,\lambda}$ is the absorption cross section for the "a" compound at a determined wavelength (cm^2 $\cdot$ molecule^{-1}), $\Phi_{a,\lambda}$ is the quantum yield (-) and λ is the wavelength for corresponding reaction (nm).

With the reaction pathway proposed above, the reaction rates for ozone and xylene as the two main reactants can be derived (Equations (30) and (31)).

$$r_{O_3} = -J_3[O_3] - J_4[O_3] - k_7[O^{\cdot}][O_3] - k_{10}[H^{\cdot}][O_3] - k_{11}[OH^{\cdot}][O_3] + k_{12}[O^{\cdot}][O_2] \tag{30}$$

$$r_{xyl} = -J_5[xyl] - k_6[xyl][OH^{\cdot}] \tag{31}$$

To calculate the concentration of short lifetime species, the following hypothesis were made: i) constant concentration of water, oxygen and nitrogen, and ii) micro steady state approximation for the radicals. The radicals are generated at the same rate that they are

consumed, so the concentration remains low and constant [38, 39]. After some algebraic work, the concentration of radicals can be expressed as follows (Eq. (32)-(34)):

$$[O\cdot] = \frac{J_2[O_2]+J_3[O_3]+J_4[O_3]}{k_7[O_3]+k_8[H_2O]+k_9[OH\cdot]+k_{12}[O_2][M]+k_{14}[N_2][M]} \quad (32)$$

$$[H\cdot] = \frac{J_1[H_2O]+k_9[OH\cdot][O\cdot]}{k_{10}[O_3]+k_{13}[O_2][M]} \quad (33)$$

$$[OH\cdot] = \frac{J_1[H_2O]+k_8[H_2O][O\cdot]+k_{10}[O_3][H\cdot]}{k_6[xyl]+k_9[O\cdot]+k_{11}[O_3]} \quad (34)$$

A radiation profile was made with laboratory measurements at 254 nm in one direction of the lamp at set distances. Using Pythagorean theorem and interpolation, a radial array of points with a lamp as a center was made. Placing these arrays to the spots like lamps in the cross-section of the reactor were placed, a simple radiation field was generated (Figure 7).

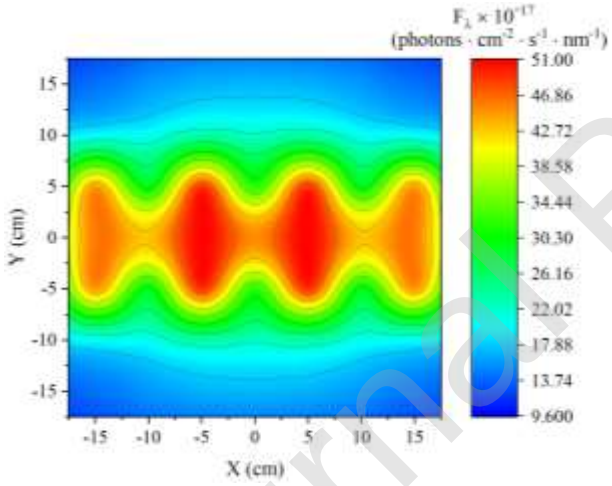

Figure 7 Radiation field at 254nm in the cross-section of the photolytic reactor (see Figure 2).

Clearly there is a major decrease of the intensity of the radiation in dependence on the distance from the light source [40]. This decrease is caused by compounds present in the air that absorb in the 254 nm wavelength and by the radial dispersion of the light. Intensity near the walls of the reactor was more than 5 times lower than in the "hot" area near the lamps. As

a consequence, overall average radiation flux at 254 nm in the whole cross-section was only 2.05×10^{18} photons $\cdot$ $cm^{-2} \cdot s^{-1} \cdot nm^{-1}$ which is not even a half value of the radiation flux near the lamps (area around the lamps up to 2.5 cm).

Xylene presents a high value of absorption cross section at 185 nm compared to other compounds (see Table 3), thus a simple dependency between the radiation flux at 185 nm and the xylene concentration was established (Equation (35)) using laboratory data.

$$F_{185}(\underline{x}) = A\exp^{BC_{xyl}(\underline{x})} \quad (35)$$

where A and B are coefficients that have to be estimated, C_{xyl} is the xylene concentration (molecule $\cdot$ cm^{-3}) and $\underline{x}$ is the position vector.

In the first approach to modelling this very complex problem, an average radiation value in the cross section area of the reactor was used. Also, diffusive and convective gradients of concentration of the components in the cross section were not considered. With these simplifications, the reactor can be modelled as one-dimensional plug flow (1D-PFR), and the resulting mass balance equation along the reactor for the main compounds is:

$$v_{air}\frac{dC_y(x)}{dx} = r_y(x) \quad (36)$$

where v_{air} is the flow velocity ($cm \cdot s^{-1}$), C is the concentration (molecule $\cdot$ cm^{-3}), "y" indicates the compound (xylene or ozone), x is the coordinate along the reactor, and r is the reaction rate (Equations (30) and (31)). The boundary conditions are:

$$C_{xyl}(0) = C_{xyl,0} \quad (37)$$

$$C_{O_3}(0) = 0 \quad (38)$$

Equation (36) was solved numerically for xylene and ozone with the Euler method, and using the photochemical parameters and reaction rate constants that are reported in literature

(Table 3). On the other hand, experimental data and the Generalized Reduced Gradient (GRG) algorithm were used to estimate the reaction rate constant k_6 corresponding to the xylene oxidation by hydroxyl radical attack and the quantum yield of xylene at 185 nm $\Phi_{xyl,185}$. The method of GRG is explained in more detail by Arora [41]. The value of k_6 was estimated as $1.19 \pm 0.17 \times 10^{-14}$ $cm^3 \cdot molecule^{-1} \cdot s^{-1}$ and the value of $\Phi_{xyl,185}$ was $5.16 \pm 0.25 \times 10^{-5}$. Also the coefficients A and B in the Equation (35) were estimated as 4.51×10^{-18} photons $\cdot cm^{-2} \cdot s^{-1} \cdot nm^{-1}$ and -3.86 $cm^3 \cdot molecule^{-1}$ respectively. The root mean square error (RMSE) of the concentrations predicted by the model and the measured ones was 3.66 % for xylene and 10.7 % for ozone.

Table 3 Data used for modeling found in literature.

Denomination	Symbol	Value	Unit	Reference
Absorption cross section	$\sigma_{xyl,185}$	1.80×10^{-16}	cm^2 $molecule^{-1}$	[42]
	$\sigma_{H2O,185}$	6.78×10^{-20}	cm^2 $molecule^{-1}$	[33]
	$\sigma_{O2,185}$	2.99×10^{-23}	cm^2 $molecule^{-1}$	[33]
	$\sigma_{O3,185}$	6.22×10^{-19}	cm^2 $molecule^{-1}$	[33]
	$\sigma_{O3,254}$	1.15×10^{-17}	cm^2 $molecule^{-1}$	[33]
Photodissociation quantum yield	$\Phi_{H2O,185}$	≥ 0.99	adim.	[33]
	$\Phi_{O2,185}$	1.00	adim.	[33]
	$\Phi_{O3,185}$	0.37	adim.	[33]
	$\Phi_{O3,254}$	0.90	adim.	[33]
Reaction rate constant	k_7	8.0×10^{-15}	cm^3 $molecule^{-1}$ s^{-1}	[33]
	k_8	2.0×10^{-10}	cm^3 $molecule^{-1}$ s^{-1}	[33]
	k_9	3.3×10^{-11}	cm^3 $molecule^{-1}$ s^{-1}	[33]
	k_{10}	2.9×10^{-11}	cm^3 $molecule^{-1}$ s^{-1}	[33]
	k_{11}	7.3×10^{-14}	cm^3 $molecule^{-1}$ s^{-1}	[33]
	k_{12}	6.0×10^{-34}	cm^6 $molecule^{-2}$ s^{-1}	[33]
	k_{13}	4.4×10^{-32}	cm^6 $molecule^{-2}$ s^{-1}	[33]
	k_{14}	2.8×10^{-36}	cm^6 $molecule^{-2}$ s^{-1}	[33]

The concentration profiles along the reactor predicted by the resolution of the mass balance (Equation (36)) and applying the kinetic model for xylene and ozone (Equations (30) and (31)) are shown in Figure 8. There is a higher xylene elimination and a higher ozone production for the lower flow rates due to a higher residence time. The elimination/production is faster up to approx. 0.5 m from the reactor inlet, then it is slowing down and graph becomes

practically linear. In theory, the complete elimination of xylene is possible if the residence time is long enough, even for relatively high concentrations.

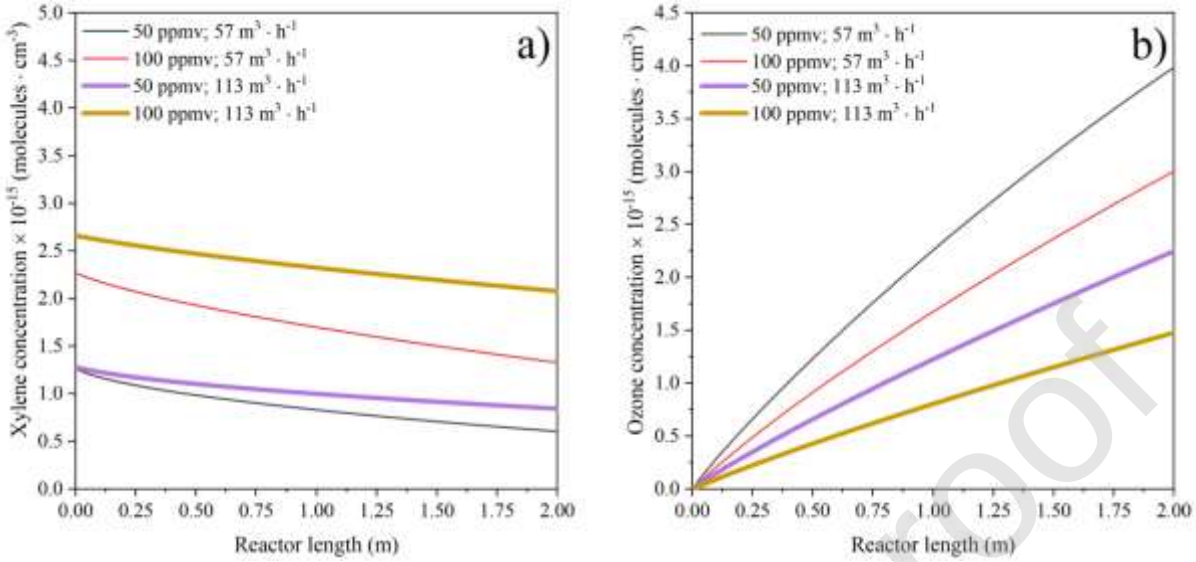

Figure 8 The model dependency of a) the xylene concentration, b) the ozone concentration on the reactor length.

The comparison between model predictions and experimental data for both xylene and ozone at the reactor outlet is shown in Figure 9.

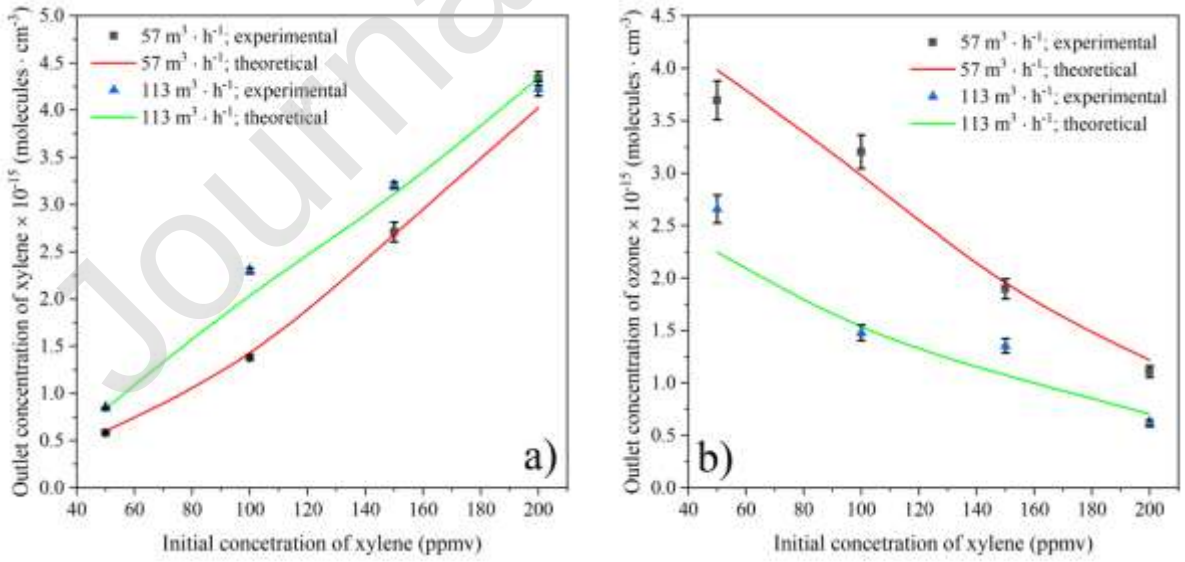

Figure 9 The comparison between model and experimental data for a) xylene, b) ozone.

As it was mentioned, xylene absorbs radiation at 185 nm, so the radiation flux depends on the xylene concentration. This has an effect on reaction rates r_1 (in a direct way) (Equation (15)) and r_8 (in an indirect way) (Equation (22)), which are the sources of $OH^{\bullet}$ radicals. On the other hand, the firstly considered reactions for xylene decomposition were: i) $OH^{\bullet}$ radical reaction (r_6), ii) photolysis (r_5), iii) direct reaction with ozone, and iv) reaction with $O^{\bullet}$ radical. In the first modeling approach, the last two reactions were calculated, but they were discarded due to the predicted low value of reaction rate constant (in orders of magnitude10^{-22} for the reaction with ozone and 10^{-13} for the reaction with $O^{\bullet}$ radical). For this work, the reaction described by Equation (20) ($OH^{\bullet}$ radical attack) is more significant than the reaction of Equation (19) (photolysis) according to the estimated values in the model. Experimental conditions tested were average 254 nm radiation flux of 2.05×10^{18} photons $\cdot$ $cm^{-2} \cdot s^{-1} \cdot nm^{-1}$ and inlet xylene concentration ranging from 50 to 200 ppm. This behavior also agrees with the work of Mohseni et al. [37]. In those experiments, the tested conditions were radiation flux at 254 nm of 3.03×10^{18} photons $\cdot$ $cm^{-2} \cdot s^{-1} \cdot nm^{-1}$ and 100 ppm of inlet xylene concentration. Thus, in these conditions, the $OH^{\bullet}$ radical attack is the main pathway for xylene degradation. However, despite the direct ozonation of xylene and the $O^{\bullet}$ radical attack can be neglected, ozone plays an important role through the formation of $OH^{\bullet}$ radicals. Finally, the initial pollutant concentration presents a chained effect on the xylene decomposition, therefore the photolysis could become more important for higher xylene concentrations.

3.4 Figures-of-merit

The important part of chemical engineering is also an economic evaluation of the whole process. For this purpose, figures-of-merit were counted so that the system can be compared to other AOPs which are widely disperse group of technologies. For this technology where the

concentration of pollutants are low, figures-of-merit were counted as an electric energy per order E_{EO} (Equation (39)) [43],

$$E_{EO} = \frac{P}{F \cdot \log \frac{c_{xyl,0}}{c_{xyl}}} \quad (39)$$

where E_{EO} is the electric energy demand for the degradation of xylene ($kW \cdot h \cdot m^{-3}$), P is the rated power (kW), F is the air flow rate ($m^3 \cdot h^{-1}$). Taking into account the most recent average prices for the electric energy per kilowatt hour for the EU (0.22 € $\cdot$ $kW^{-1} \cdot h^{-1}$, 2019) the cost for one-hour treatment of the waste gas would not exceed 6.73 € as seen in Table 4 and 5.

Table 4 E_{EO} and electric energy cost summary for the flow rate 57 $m^3 \cdot h^{-1}$.

Average inlet concentration (ppmv)	Average concentration after R1 (ppmv)	Average outlet concentration (ppmv)	E_{EO} for R1 ($kW \cdot h \cdot m^{-3}$)	Cost (€ $\cdot$ m^{-3})	E_{EO} for R1+R2 ($kW \cdot h \cdot m^{-3}$)	Cost (€ $\cdot$ m^{-3})
51.33	25.17	2.33	0.075	0.016	0.046	0.010
100.33	62.11	22.78	0.111	0.024	0.097	0.021
153.58	124.15	93.75	0.251	0.055	0.290	0.064
213.17	188.00	163.33	0.424	0.093	0.538	0.118

Table 5 E_{EO} and electric energy cost summary for the flow rate 113 $m^3 \cdot h^{-1}$.

Average inlet concentration (ppmv)	Average concentration after R1 (ppmv)	Average outlet concentration (ppmv)	E_{EO} for R1 ($kW \cdot h \cdot m^{-3}$)	Cost (€ $\cdot$ m^{-3})	E_{EO} for R1+R2 ($kW \cdot h \cdot m^{-3}$)	Cost (€ $\cdot$ m^{-3})
52.34	34.67	10.83	0.065	0.014	0.046	0.010
113.33	97.55	72.22	0.179	0.039	0.160	0.035
154.32	135.11	98.78	0.202	0.045	0.162	0.036
208.00	184.21	145.17	0.221	0.049	0.201	0.044

From the economic point of view, this AOPs technology is more suitable for the higher flow rate (113 $m^3 \cdot h^{-1}$) where the prices for one-hour treatment are lower than for the flow rate

57 $m^3 \cdot h^{-1}$. In the case of the highest measured inlet concentration of xylene (approximately 200 ppmv), the cost of reducing the xylene concentration by an order of magnitude at a higher flow rate (113 $m^3 \cdot h^{-1}$) is almost 3 times lower than at flow rate 57 $m^3 \cdot h^{-1}$. Furthermore, more economically advantageous is the use of both steps (R1 + R2) of the technology, despite the fact that energy consumption by the whole unit is nearly 3 times higher than by using only the first step, but the eliminated amount of pollutant is nearly two times higher.

4. Conclusions

A pilot plant technology using advanced oxidation processes was successfully tested for the elimination of xylene from waste gases. Both steps of the unit, photolytic and photochemical reactor showed their effectivity towards elimination of xylene. The highest conversion (95 %) of xylene was achieved for the flow rate 57 $m^3 \cdot h^{-1}$ and initial concentration of xylene 50 ppmv. Needless to say, after calculating the figures-of-merit, the higher flow rate 113 $m^3 \cdot h^{-1}$ was more economically advantageous, where the cost for one-hour treatment of the waste gas was 0.044 € $\cdot m^{-3}$ for the initial concentration of xylene 200 ppmv. In addition to the experimental data modeling was calculated as well. Modeling showed that xylene is eliminated mainly due to its reaction with hydroxyl radicals, which are formed both by the reaction of ozone with water but also by the reaction of singlet oxygen (formed by the decomposition of ozone) with water. It also showed that it is theoretically possible to achieve 100% elimination of xylene, if the reactor is long enough. This idea is supported by graphical results of model in which the concentration dependencies of xylene become practically linear. With the actual design, the unit is more suitable for lower flow rates and with some changes it can be a good alternative for the actual technologies for the waste gas treatment.

Author contributions

T.P. and T.K. performed the measurements, M.R., R.Ž. and K.K. were involved in planning and supervised the work, T.P. and F.S. drafted the manuscript, F.S. and M.M.B made the mathematical modeling part, T.P, M.R., F.S., M.M.B. and K.K reviewed the manuscript and made amendments. All authors contributed with their expertise and hard work.

Declaration of interests

The authors declare that they have no known competing financial interests or personal relationships that could have appeared to influence the work reported in this paper.

Acknowledgements

This work was supported by EU structural funding in Operational Programme Research, Development and Education, project No. CZ.02.1.01./0.0/0.0/17_049/0008419 "COOPERATION" and by using Large Research Infrastructure ENREGAT supported by the Ministry of Education, Youth and Sports of the Czech Republic under project No. LM2018098.

References

[1] Y.-H. Chuang, A. Szczuka, F. Shabani, J. Munoz, R. Aflaki, S.D. Hammond, W.A. Mitch, Pilot-scale comparison of microfiltration/reverse osmosis and ozone/biological activated carbon with UV/hydrogen peroxide or UV/free chlorine AOP treatment for controlling disinfection byproducts during wastewater reuse, Water Res. 152 (2019) 215-225. https://doi.org/10.1016/j.watres.2018.12.062.

[2] L. Sbardella, I. Velo Gala, J. Comas, S. Morera Carbonell, I. Rodríguez-Roda, W. Gernjak, Integrated assessment of sulfate-based AOPs for pharmaceutical active compound removal from wastewater, J. Clean. Prod. 260 (2020) 121014. https://doi.org/10.1016/j.jclepro.2020.121014.

[3] C. Wang, M. Hofmann, A. Safari, I. Viole, S. Andrews, R. Hofmann, Chlorine is preferred over bisulfite for H_2O_2 quenching following UV-AOP drinking water treatment, Water Res. 165 (2019) 115000. https://doi.org/10.1016/j.watres.2019.115000.

[4] N. Wardenier, Z. Liu, A. Nikiforov, S.W.H. Van Hulle, C. Leys, Micropollutant elimination by O_3, UV and plasma-based AOPs: An evaluation of treatment and energy costs, Chemosphere 234 (2019) 715-724. https://doi.org/10.1016/j.chemosphere.2019.06.033.

[5] K. Kočí, M. Reli, I. Troppová, T. Prostějovský, R. Žebrák, Degradation of Styrene from Waste Gas Stream by Advanced Oxidation Processes, Clean-Soil Air Water 47 (2019) 1900126. https://doi.org/10.1002/clen.201900126.

[6] R. Hao, Z. Wang, X. Mao, Y. Gong, B. Yuan, Y. Zhao, B. Tian, M. Qi, Elemental mercury removal by a novel advanced oxidation process of ultraviolet/chlorite-ammonia: Mechanism and kinetics, J. Hazard. Mater. 374 (2019) 120-128. https://doi.org/10.1016/j.jhazmat.2019.03.134.

[7] J. Chen, Y. Huang, G. Li, T. An, Y. Hu, Y. Li, VOCs elimination and health risk reduction in e-waste dismantling workshop using integrated techniques of electrostatic precipitation

with advanced oxidation technologies, J. Hazard. Mater. 302 (2016) 395-403. https://doi.org/10.1016/j.jhazmat.2015.10.006.

[8] C. Yang, G. Miao, Y. Pi, Q. Xia, J. Wu, Z. Li, J. Xiao, Abatement of various types of VOCs by adsorption/catalytic oxidation: A review, Chem. Eng. 370 (2019) 1128-1153. https://doi.org/10.1016/j.cej.2019.03.232.

[9] P.T.J. Scheepers, L. de Werdt, M. van Dael, R. Anzion, J. Vanoirbeek, R.C. Duca, M. Creta, L. Godderis, D.T.D. Warnakulasuriya, N.M. Devanarayana, Assessment of exposure of gas station attendants in Sri Lanka to benzene, toluene and xylenes, Environ. Res. 178 (2019) 108670. https://doi.org/10.1016/j.envres.2019.108670.

[10] M. Zang, C. Zhao, Y. Wang, S. Chen, A review of recent advances in catalytic combustion of VOCs on perovskite-type catalysts, J. Saudi Chem. Soc. 23 (2019) 645-654. https://doi.org/10.1016/j.jscs.2019.01.004.

[11] L.M. McKenzie, R.Z. Witter, L.S. Newman, J.L. Adgate, Human health risk assessment of air emissions from development of unconventional natural gas resources, Sci. Total Environ. 424 (2012) 79-87. https://doi.org/10.1016/j.scitotenv.2012.02.018.

[12] A. Garg, N.C. Gupta, S.K. Tyagi, Levels of Benzene, Toluene, Ethylbenzene, and Xylene near a Traffic-Congested Area of East Delhi, Environ. Claims J. 31 (2019) 5-15. https://doi.org/10.1080/10406026.2018.1525025.

[13] R. Ravi, R. Narendiran, K. Kauselya, Biofiltration Emerging Technology for Removal of Volatile Organic Compounds (VOC's) - A Review, Int. J. Energy Environ. 10 (2015) 1-8.

[14] K. Lelicińska-Serafin, A. Rolewicz-Kalińska, P. Manczarski, VOC Removal Performance of a Joint Process Coupling Biofiltration and Membrane-Filtration Treating Food Industry Waste Gas, Int. J. Environ. Res. Public Health 16 (2019) 3009. https://doi.org/10.3390/ijerph16173009.

[15] A. Tiwari, T. Alam, A. Kumar, A. Shukla, Control of Odour, Volatile Organic Compounds (VOCs) & Toxic Gases through Biofiltration-An Overview, International Conference on Modern Trends in Civil Engineering (Towards Sustainable Development Goals), 2019.

[16] W.B. Li, J.X. Wang, H. Gong, Catalytic combustion of VOCs on non-noble metal catalysts, Catal. Today 148 (2009) 81-87. https://doi.org/10.1016/j.cattod.2009.03.007.

[17] M. Tomatis, H.-H. Xu, J. He, X.-D. Zhang, Recent Development of Catalysts for Removal of Volatile Organic Compounds in Flue Gas by Combustion: A Review, J. Chem. 2016 (2016) 15. https://doi.org/10.1155/2016/8324826.

[18] M. Ouzzine, A.J. Romero-Anaya, M.A. Lillo-Ródenas, A. Linares-Solano, Spherical activated carbons for the adsorption of a real multicomponent VOC mixture, Carbon 148 (2019) 214-223. https://doi.org/10.1016/j.carbon.2019.03.075.

[19] K. Pui Wee, R. Yusoff, K. Aroua Mohamed, A review on activated carbon adsorption for volatile organic compounds (VOCs), Rev. Chem. Eng. 35 (2019) 649. https://doi.org/10.1515/revce-2017-0057.

[20] D.M. Kempisty, R.S. Summers, G. Abulikemu, N.V. Deshpande, J.A. Rebholz, K. Roberts, J.G. Pressman, Granular activated carbon adsorption of carcinogenic volatile organic compounds at low influent concentrations, AWWA Water Sci. 1 (2019) e1128. https://doi.org/10.1002/aws2.1128.

[21] L. Liu, J. Li, H. Zhang, L. Li, P. Zhou, X. Meng, M. Guo, J. Jia, T. Sun, In situ fabrication of highly active γ-MnO_2/$SmMnO_3$ catalyst for deep catalytic oxidation of gaseous benzene, ethylbenzene, toluene, and o-xylene, J. Hazard. Mater. 362 (2019) 178-186. https://doi.org/10.1016/j.jhazmat.2018.09.012.

[22] R. Rashidi, G. Moussavi, A. Khavanin, A. Ghaderpoori, The efficacy of the ozonation process in the presence of activated carbon impregnated with magnesium oxide in the removal

of benzene from the air stream, Int. J. Environ. Sci. Technol. 16 (2019) 8023–8030. https://doi.org/10.1007/s13762-019-02239-0.

[23] H. Ali Rangkooy, F. Jahani, A. Siahi Ahangar, Effect of the Type of Ultraviolet on the Photocatalytic Removal of Xylene as a Pollutant in the Air Using TiO_2 Nanoparticles Fixed on the Activated Carbon, J. Occup. Hyg. Eng. 5 (2019) 26-32. https://doi.org/10.29252/johe.5.4.26.

[24] P.D. Cooper, R.E. Johnson, T.I. Quickenden, A review of possible optical absorption features of oxygen molecules in the icy surfaces of outer solar system bodies, Planet. Space Sci. 51 (2003) 183-192. https://doi.org/10.1016/S0032-0633(02)00205-2.

[25] R. Munter, Advanced Oxidation Processes: Current status, Proc. Estonian Acad. Sci. Chem. 50 (2001) 59-80.

[26] M.S. Johnson, E.J.K. Nilsson, E.A. Svensson, S. Langer, Gas-Phase Advanced Oxidation for Effective, Efficient in Situ Control of Pollution, Environ. Sci. Technol. 48 (2014) 8768-8776. https://doi.org/10.1021/es5012687.

[27] R. Atkinson, J. Arey, Atmospheric Degradation of Volatile Organic Compounds, Chem. Rev. 103 (2003) 4605-4638. https://doi.org/10.1021/cr0206420.

[28] J.M. Andino, J.N. Smith, R.C. Flagan, W.A. Goddard, J.H. Seinfeld, Mechanism of Atmospheric Photooxidation of Aromatics: A Theoretical Study, The Journal of Physical Chemistry 100 (1996) 10967-10980. https://doi.org/10.1021/jp952935l.

[29] R. Atkinson, S.M. Aschmann, J. Arey, Formation of ring-retaining products from the OH radical-initated reactions of o-, m-, and p-xylene, Int. J. Chem. Kinet. 23 (1991) 77-97. https://doi.org/10.1002/kin.550230108.

[30] H.M. Lee, M.B. Chang, Abatement of Gas-phase p-Xylene via Dielectric Barrier Discharges, Plasma Chem. Plasma P. 23 (2003) 541-558. https://doi.org/10.1023/A:1023239122885.

[31] Z. Fan, P. Lioy, C. Weschler, N. Fiedler, H. Kipen, J. Zhang, Ozone-Initiated Reactions with Mixtures of Volatile Organic Compounds under Simulated Indoor Conditions, Environ. Sci. Technol. 37 (2003) 1811-1821. https://doi.org/10.1021/es026231i.

[32] T. Oppenländer, Photochemical Purification of Water and Air. Advanced Oxidation Processes (AOPs): Principles, Reaction Mechanisms, Reactor Concepts, Wiley-VCH, Verlag, 2003.

[33] J.B. Burkholder, S.P. Sander, J. Abbatt, J. Barker, R. Huie, C.E. Kolb, M. Kurylo, V. Orkin, D.M. Wilmouth, P. Wine, Chemical Kinetics and Photochemical Data for Use in Atmospheric Studies, Evaluation Number 18, Jet Propulsion Laboratory, National Aeronautics and Space Administration, Pasadena, California, 2015.

[34] L. Furatian, M. Mohseni, Temperature dependence of 185 nm photochemical water treatment – The photolysis of water, J. Photoch. Photobio. A 356 (2017) 364-369. https://doi.org/10.1016/j.jphotochem.2017.12.030.

[35] K. Zoschke, H. Börnick, E. Worch, Vacuum-UV radiation at 185 nm in water treatment--a review, Water Res. 52 (2014) 131-145. https://doi.org/10.1016/j.watres.2013.12.034.

[36] L. Yang, M. Li, W. Li, J. Bolton, Z. Qiang, A Green Method to Determine VUV (185 nm) Fluence Rate Based on Hydrogen Peroxide Production in Aqueous Solution, Phtotochem. Photobiol. 94 (2018) 821-824. https://doi.org/10.1111/php.12913.

[37] M. Mohseni, L.-H. Koh, D. Kuhn, D. Allen, Ultraviolet photooxidation for the biodegradability enhancement of airborne o-xylene, J. Environ. Eng. Sci. 4 (2005) 279-286. https://doi.org/10.1139/s04-060.

[38] O.M. Alfano, M.a.I. Cabrera, A.E. Cassano, Photocatalytic Reactions Involving Hydroxyl Radical Attack, J. Catal. 172 (1997) 370-379. https://doi.org/10.1006/jcat.1997.1858.

[39] M.d.l.M. Ballari, M.L. Satuf, O.M. Alfano, Photocatalytic Reactor Modeling: Application to Advanced Oxidation Processes for Chemical Pollution Abatement, Top. Curr. Chem. 377 (2019) 22. https://doi.org/10.1007/s41061-019-0247-2.

[40] N. Voudoukis, S. Oikonomidis, Inverse square law for light and radiation: A unifying educational approach, EJERS 2 (2017) 23-27. https://doi.org/10.24018/ejers.2017.2.11.517.

[41] J.S. Arora, Chapter 13 - More on Numerical Methods for Constrained Optimum Design, in: J.S. Arora (Ed.) Introduction to Optimum Design (Fourth Edition), Academic Press, Boston, 2017, pp. 555-599.

[42] M. Suto, X. Wang, J. Shan, L.C. Lee, Quantitative photoabsorption and fluorescence spectroscopy of benzene, naphthalene, and some derivatives at 106–295 nm, J. Quant. Spectrosc. Ra. 48 (1992) 79-89. https://doi.org/10.1016/0022-4073(92)90008-R.

[43] J. Bolton, K. Bircher, W. Tumas, C.A. Tolman, Figures-of-Merit for the Technical Development and Application of Advanced Oxidation Technologies for both Electric- and Solar-Driven Systems, Pure Appl. Chem. 73 (2001) 617-637. https://doi.org/10.1351/pac200173040627.